Geotechnical Testing Journal

doi:10.1520/GTJ20200236 available online at www.astm.org

Cristian Yair Soriano Camelo,[1] Maria Cascão Ferreira de Almeida,[2] S. P. Gopal Madabhushi,[3] Sam A. Stanier,[4] Marcio de Souza Soares de Almeida,[5] Huida Liu,[6] and Ricardo Garske Borges[7]

Seismic Centrifuge Modeling of a Gentle Slope of Layered Clay, Including a Weak Layer

Reference

C. Y. Soriano Camelo, M. C. F. de Almeida, S. P. G. Madabhushi, S. A. Stanier, M. S. S. de Almeida, H. Liu, and R. G. Borges, "Seismic Centrifuge Modeling of a Gentle Slope of Layered Clay, Including a Weak Layer," *Geotechnical Testing Journal* https://doi.org/10.1520/GTJ20200236

ABSTRACT

This article presents a model preparation methodology for simulating the seismic behavior of a gentle slope in clay with the presence of a soft, weak layer employing centrifuge testing. The model consisted of a three-layered slope of relatively soft clay with a 3° inclination, representative of Brazilian marine subsoils. In-flight characterization of the undrained shear strength and shear wave velocity profiles were achieved through T-bar penetrometer and air hammer tests. The model was subjected to a series of earthquake simulations at different amplitudes, and the response was tracked with accelerometers and displacement transducers. Additional data were obtained using a particle image velocimetry (PIV) methodology also described in this work. The results show that the proposed model preparation methodology enables the simulation of the strength contrast between the weak and relatively stronger surrounding layers using a laminar container. The additional displacement and acceleration data obtained from the PIV were in good agreement with the corresponding displacement transducer and accelerometer measurements. From the spectral analysis, a shift in the fundamental period was observed as the strain amplitude was increased, suggesting that strain rate effects mobilize higher stresses and a strength rate correction should be considered for the calibration of numerical models and comparison with existing methods for calculation of dynamic displacements in slopes.

Keywords

seismic response, centrifuge modeling, soft clay, submarine slope, weak layer

Manuscript received August 24, 2020; accepted for publication May 10, 2021; published online July 9, 2021.

[1] Graduate School of Engineering, Instituto Alberto Luiz Coimbra de Pós-Graduação e Pesquisa de Engenharia (COPPE), Federal University of Rio de Janeiro, Avenida Pedro Calmon, Laboratorio Geotecnia- Anexo Engeharia Civil- Cidade Universitária, Rio de Janeiro 21941596, Brazil (Corresponding author), e-mail: cysorianoc@coc.ufrj.br, https://orcid.org/0000-0001-9530-0185

[2] Polytechnic School of Engineering - Poli, Federal University of Rio de Janeiro, Avenida Athos da Silveira Ramos, 149, Centro de Tecnologia - Bloco A, 2° andar - sala 5, Cidade Universitária, Rio de Janeiro 21941596, Brazil, https://orcid.org/0000-0002-3133-6098

[3] University of Cambridge, Schofield Centre, High Cross Madingley Rd., Cambridge CB3 0EF, UK, https://orcid.org/0000-0003-4031-8761

[4] Department of Engineering, University of Cambridge, Trumpington St., Cambridge CB2 1PZ, UK, https://orcid.org/0000-0001-5671-2902

[5] Instituto Alberto Luiz Coimbra de Pós-Graduação e Pesquisa de Engenharia (COPPE), Federal University of Rio de Janeiro, Avenida Pedro Calmon, Laboratorio Geotecnia-Anexo Engenharia Civil- Cidade Universitária, Rio de Janeiro 21941596, Brazil, https://orcid.org/0000-0003-2230-397X

[6] China Construction Infrastructure Co., Ltd., Chegongzhuang St., Xicheng District, Beijing 100044, China

[7] Petrobras, Centro de Pesquisa e Desenvolvimento Leopoldo Américo Miguez de Mello (CENPES), Av. Horácio Macedo, 950 - Cidade Universitária da Universidade Federal do Rio de Janeiro, Rio de Janeiro 21941915, Brazil, https://orcid.org/0000-0001-7623-0337

Introduction

The continental slope in the southern and southeastern regions of Brazil is relatively uniform over long distances, being disturbed only by some widely spaced surface geological features. In the Campos Basin, located on the continental margin of Southeastern Brazil, pelagic and hemipelagic sedimentation are predominant, with an average accumulation rate of 0.064 m/1,000 years (Kowsmann, Lima, and Vicalvi 2016). The deposition of fine materials at such low rates leads to the formation of parallel layers of normally consolidated to lightly overconsolidated, soft cohesive deposits ranging in depth from a few meters to hundreds of meters (Biscontin and Pestana 2006). The slope inclination in those cases is small with typical values of less than 5°. These slopes are theoretically stable under gravity loads because of strength gains during the low rates of sedimentation of the materials. However, large-scale submarine landslides around the world have occurred in slopes with similarly low gradients (Hühnerbach and Masson 2004).

In such offshore areas with low sedimentation rates, earthquakes are one of the primary catalysts for submarine landslides (Nadim, Biscontin, and Kaynia, n.d.). In addition, variable rates of deposition of submarine sediments may lead to the generation of weak layers with varying degrees of consolidation (Biscontin, Pestana, and Nadim 2004). Several studies related to submarine mass movements have suggested the presence of weak layers as one of the causes of the triggering of submarine landslides (O'Leary 1991; Haflidason et al. 2003; Bryn et al. 2005a, 2005b; Solheim et al. 2005; Locat and Lee 2009).

Earthquakes of moderate to large magnitudes do not frequently occur along the Brazilian continental margin; however, earthquakes with damage potential have occurred in the past and may occur again (Pirchiner et al., n.d.; Borges et al. 2020). Recent studies have focused on the occurrence of hydroplaning and turbidity currents (Acosta et al. 2017; Hotta et al. 2020), on the response of clayey submarine canyons to seismic events representative of Brazilian seismicity (Tarazona et al. 2020), and also on the assessment of seismic hazard on the continental margin of southeastern Brazil (Borges et al. 2020). However, the seismic response of submarine slopes in the Brazilian context is a new field of investigation. This study comprises part of a research project related to the seismic behavior of low-gradient (<5°), soft-clay continental slopes typical of this region.

In the case of submarine slopes, landslides involve large distances relative to the thickness of the soil mass. Therefore, the length of the slide is many times larger than the thickness of the slide. The infinite slope approach to modeling the seismic response of sloping ground in soft clays has been studied by means of numerical models in several studies (Pestana and Nadim 2000; Biscontin and Pestana 2006; Rodríguez-Ochoa et al. 2015; Zhou, Chen, She, et al. 2017; Dey et al. 2016). However, field or experimental data regarding the seismic behavior of gentle slopes in soft clays under different ranges of loading are limited. Most of the experimental studies in clays, particularly using centrifuge modeling, have been related to one-dimensional (1D) response at different ranges of strain. For example, Afacan, Brandenberg, and Stewart (2014) performed 1D centrifuge tests in clay using a hinged-plate model container to evaluate the site response at very large strains representative of seismically active regions. In another study, Rayhani and El Naggar (2007) evaluated the seismic response of soft to medium stiff clays of one and two layers using an equivalent shear beam (ESB) model container. More recently, Zhou, Chen, Chen, et al. (2017) carried out a series of centrifuge tests on a slightly overconsolidated marine clay deposit employing a flexible boundary container.

In the case of lateral spreading problems like the seismic behavior of sloping ground, the use of ESB model containers is unsuitable given that they restrain the lateral

displacements of the soil (Madabhushi 2014). Alternatively, a laminar container can be used for this type of problem. Most of the experience using laminar containers in centrifuge tests is related to liquefaction problems (Elgamal et al. 1996; Taboada and Dobry 1998; Haigh et al. n.d.; Knappett 2006).

One of the fundamental concerns of the preparation of models in clay is the consolidation of the soil. This requires the use of an impermeable container strong enough to handle the pressures applied to the clay during consolidation. In a laminar container, the soil body is typically placed within a rubber bag or a latex membrane for saturated models. For the construction of a layered profile in clay, an extension is required, and the inner rubber bag can be easily damaged during the application of the consolidation pressures, leading to leakage and the generation of additional drainage paths. To sort out these practical issues, it was necessary to develop a new model preparation procedure.

This article presents an experimental methodology to simulate the seismic behavior of a gentle slope in soft clay including the presence of a weak layer by means of centrifuge modeling. The centrifuge test presented here is part of an experimental program aimed at studying the seismic response of gentle slopes in soft clay. The specific objectives of the present work are (1) to describe a novel model-preparation technique for simulating a slope of relatively soft clay with an even weaker layer sandwiched between, using a laminar model container used extensively for seismic studies in sands (Lanzano et al. 2012; Brennan, Madabhushi, and Houghton n.d.; Tricarico, Madabhushi, and Aversa 2016; García-Torres and Madabhushi 2019), (2) to present a particle image velocimetry (PIV) methodology using an open source software (Blender) as a complementary source of data in terms of displacements and accelerations at different depths in the slope, (3) to discuss the experimental results for use in calibration of numerical and analytical models, and (4) to observe the dynamic behavior of the slope using spectral analysis.

Dynamic Centrifuge Modeling

Centrifuge modeling enables the study of complex geotechnical problems using small-scale models, employing centrifugal acceleration to simulate the stress and strains representative of field conditions (Taylor 1995; Madabhushi 2014). The dynamic tests in this study were conducted in the 10-m-diameter beam centrifuge at the Schofield Centre (University of Cambridge). The earthquake motions were applied using a servo-hydraulic actuator developed by Madabhushi et al. (2012). The problem studied consisted of a semi-infinite sloping ground condition in soft clay. Under these conditions, large deformations are expected and therefore a laminar container (Brennan, Madabhushi, and Houghton n.d.) was used. The box is 500 by 250 mm in length and width, and the depth is variable, depending on the number of rectangular frames (laminae) used (280 mm for the current centrifuge test).

Materials and Methods

MATERIALS

The model was made with Speswhite kaolin, a well-documented material with comparative data sets available and widely used in research projects involving physical models (Almeida 1984; Kim 1996; Williamson 2014; Lau 2015). For the current research, the values reported by Lau (2015), for a plastic limit (PL) equal to 30 % and a liquid limit (LL) equal to 63 % (then a plasticity index [PI] of 33 %) were adopted.

PROPOSED MODEL PREPARATION

The centrifuge test performed simulates the behavior of a layered gentle slope in soft clay when subjected to earthquake loading. The model consisted of a three-layer slope with a weak layer, aiming to simulate a strength contrast of about 25 % between neighboring layers. The consolidation pressures described below (250 and 125 kPa) were selected to reproduce a strength profile typical of marine clays like that encountered in the seabed of the Campos offshore basin, southeastern Brazil. Fagundes et al. (2012) described the behavior of marine clays in this region through laboratory and field tests and presented a profile with values ranging between 3 kPa at the surface and 40 kPa at a 20-m depth, approximately the prototype vertical extent as presented in the following sections. Similar consolidation pressures such as those used in the current test have been applied in centrifuge

tests in soft clay representative of offshore environments (White, Gaudin, and Boylan 2010; Tarazona et al. 2020). The main difference in the construction of the model presented in this article is the lower consolidation pressure of 125 kPa in order to consider the presence of a weak layer.

The model soil profile was built from reconstituted clay. The laminar container at the Schofield Centre has been used extensively for liquefaction and lateral spreading problems involving sands. For a model in clay, a different setup was required for the consolidation process. A strongbox, or consolidation container, was designed with the same internal dimensions as the laminar container (500-mm length by 250-mm width), but deeper (500 mm), aiming to produce samples of the clay between 250 and 300 mm in height at the end of consolidation. The sides of the consolidation container can be easily detached, and complete slices of the consolidated clay can be removed with minimal disturbance, enabling the simulation of the target layered soil profile as described below.

In order to build the three-layer slope, the model preparation was divided into stages:

(1) the kaolin powder was mixed with water at 120 % water content employing a clay mixer under vacuum to remove air bubbles from the clay. Once mixed, the slurry was poured into the consolidation container with draining interfaces at the top and base of the clay. A piston was placed on top of the clay slurry and it was left to consolidate for one day under the weight of the piston. The additional consolidation pressures were applied in stages using a computer-controlled consolidation rig.

(2) The top and bottom layers of the clay were first consolidated by applying a maximum consolidation pressure of $\sigma'_{v\,\max} = 250$ kPa. The load was applied in steps, starting from 0.7 kPa, corresponding to the pressure applied by the piston and increased by doubling the pressures until reaching 250 kPa. The time intervals of each loading step followed the experience of the last 40 years using Speswhite kaolin. The consolidation lasted twelve days, and it was stopped when the settlements were stabilized within 48 h (**fig. 1*A***). During the initial stages of consolidation (day 0 to day 4), a combination of consolidation of the

FIG. 1 Model consolidation stages: (*A*) consolidation of top and bottom layers; (*B*) removing and storing of the top block of the clay; (*C*) pouring of a new layer of slurry; (*D*) consolidation of the weak layer; (*E*) the stored block is positioned back and the three-layer clay is reconsolidated; (*F*) removal of the reconsolidation pressure and the three-layer clay profile is ready for the installation of the laminar container frames.

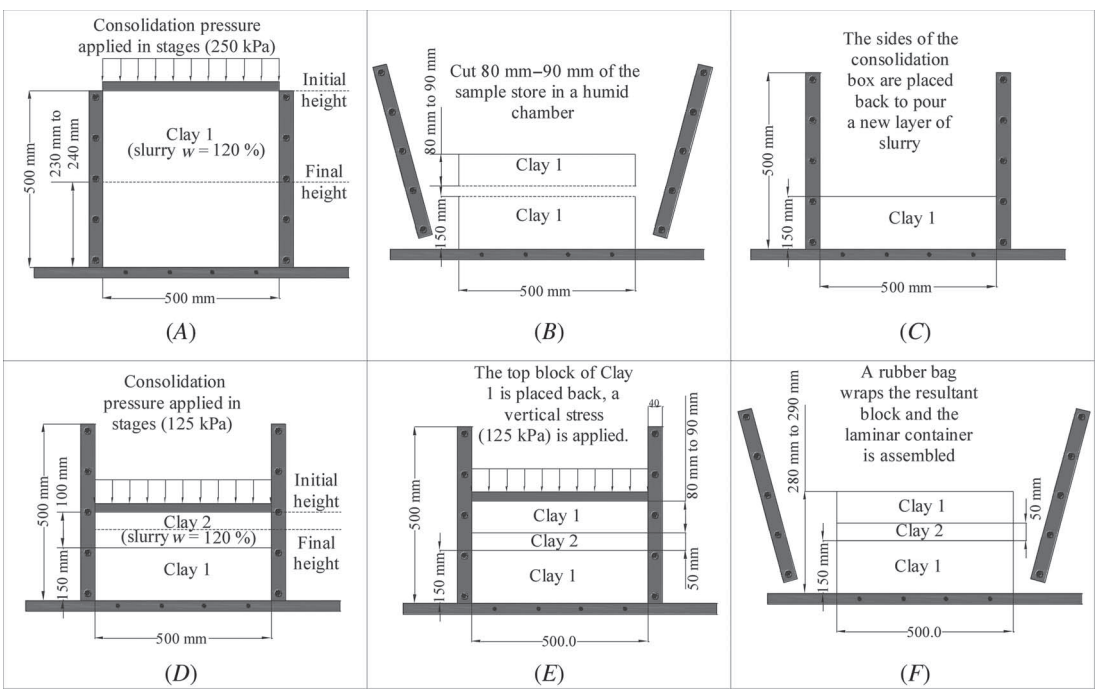

vertical stress applied by the consolidation press and suction-induced seepage were used to consolidate the clay slurry and to accelerate the settlements. This methodology has been used for models in clay developed at the Schofield Centre (Garala and Madabhushi 2019; de Sanctis et al. 2021).

(3) The sides of the consolidation container were removed; the resultant block was split by cutting off the top 80 mm and keeping the remaining 150 mm in the same position. The top block was stored and protected to avoid loss of moisture (**fig. 1B**).

(4) The sides of the consolidation container were reassembled, and a new layer of the slurry was poured on top of the block of consolidated clay that remained, then, a maximum consolidation pressure of $\sigma'_{v\,\max} =$ 125 kPa was applied in stages. The consolidation pressures were applied in 10 days in stages from 0.7 kPa doubling the pressures until reaching 125 kPa (**fig. 1C** and **1D**).

(5) At the end of the consolidation of the second layer, the previously stored top layer was positioned on top, and a $\sigma'_{v\,\max} = 125$ kPa pressure was applied to the three-layer clay bed for two days to ensure continuity between layers (**fig. 1E**). The continuity between the layers was checked after the centrifuge test by cutting transverse slices of clay, further details are presented in the post-test investigations section of this article.

(6) The applied vertical pressure was removed, and the sides of the consolidation container were again detached. Then the final block of clay was wrapped in a rubber bag to prevent water leakage and to separate the clay and the laminations (**fig. 1F**). Finally, the frames of the laminar container were assembled around the sample.

Considering that after unloading the clay, there would be a reduction in the effective stress prior to centrifuge testing commencing, the clay was held under a suction of around −60 kPa. This was done by connecting a vacuum pump to the drains located at the base of the model container (**fig. 2A**), allowing for a continuous application of negative pressure until the moment prior to the centrifugal acceleration of the model in the centrifuge. The applied suction of −60 kPa was below the air entry value to prevent the occurrence of cavitation. A range of pressures of the same order (−60 to −70 kPa) was used by Garala, Madabhushi, and Di Laora (forthcoming) and de Sanctis et al. (2021) for the preparation of models in clay during the unloading phase of consolidation. Given the short time in which the suction was applied to the model, no considerable effects were expected in terms of the saturation of the clay. As part of the experimental setup, water content samples were taken at different depths across the clay profile at the end of the centrifuge test. The average water content and degree of saturation of the clay were around 53 % and 100 %, respectively, confirming that during the centrifuge test the clay was in a saturated condition. For the calculations of the vertical stresses, two saturated unit weights were measured: for the top and bottom layer $\gamma_{sat} = 16.9$ kN/m^3 and for the weak layer $\gamma_{sat} = 16.4$ kN/m^3.

MODEL DETAILS: GENTLE SLOPE

Once assembled to the desired height, the instrumentation was installed in the laminar container. The following electronic instruments were used: (1) piezoelectric accelerometers (model A32 by D. J. Birchall Ltd.) to record the dynamic motions at different locations in the soil profile; (2) pore pressure transducers (PPTs, model PDCR-81 manufactured by Druck Ltd.); (3) linear variable differential transformers (LVDTs, model DC15 manufactured by Solartron Metrology) to record the horizontal displacements during the swing-up of the model and during the application of the dynamic loads and (4) a high-speed camera (MotionBLITZ EoSens mini 2 produced by Mikrotron GmbH) to track the displacements of markers installed in the laminae throughout the experiment. In addition, a support gantry frame was used to fix an actuator above the clay that was used to perform an in-flight T-bar test, and an air hammer device (AHD) was placed on the clay surface. The piezo-accelerometers (A1 to A10) and the PPTs (P1 to P4) were installed by excavating boreholes with small pipes, removing the clay and positioning the instruments with a probe for installation at specific depths (Brennan, Madabhushi, and Cooper n.d.). **Figure 2A** presents a general view of the model, **figure 2B** shows the detailed location of the instrumentation, and **figure 3** displays a view of the model in the servo-hydraulic actuator and the wiring arrangement in the model.

PIV ANALYSIS SETUP

For the experiment, a high-speed camera developed to record fast processes in confined spaces was employed (MotionBLITZ EoSens mini 2 produced by Mikrotron). The resolution of the pictures captured by the camera is

FIG. 2 Experimental setup: (*A*) 3D overview of the model (drawing in model scale) and (*B*) instrumentation layout (model scale in parentheses).

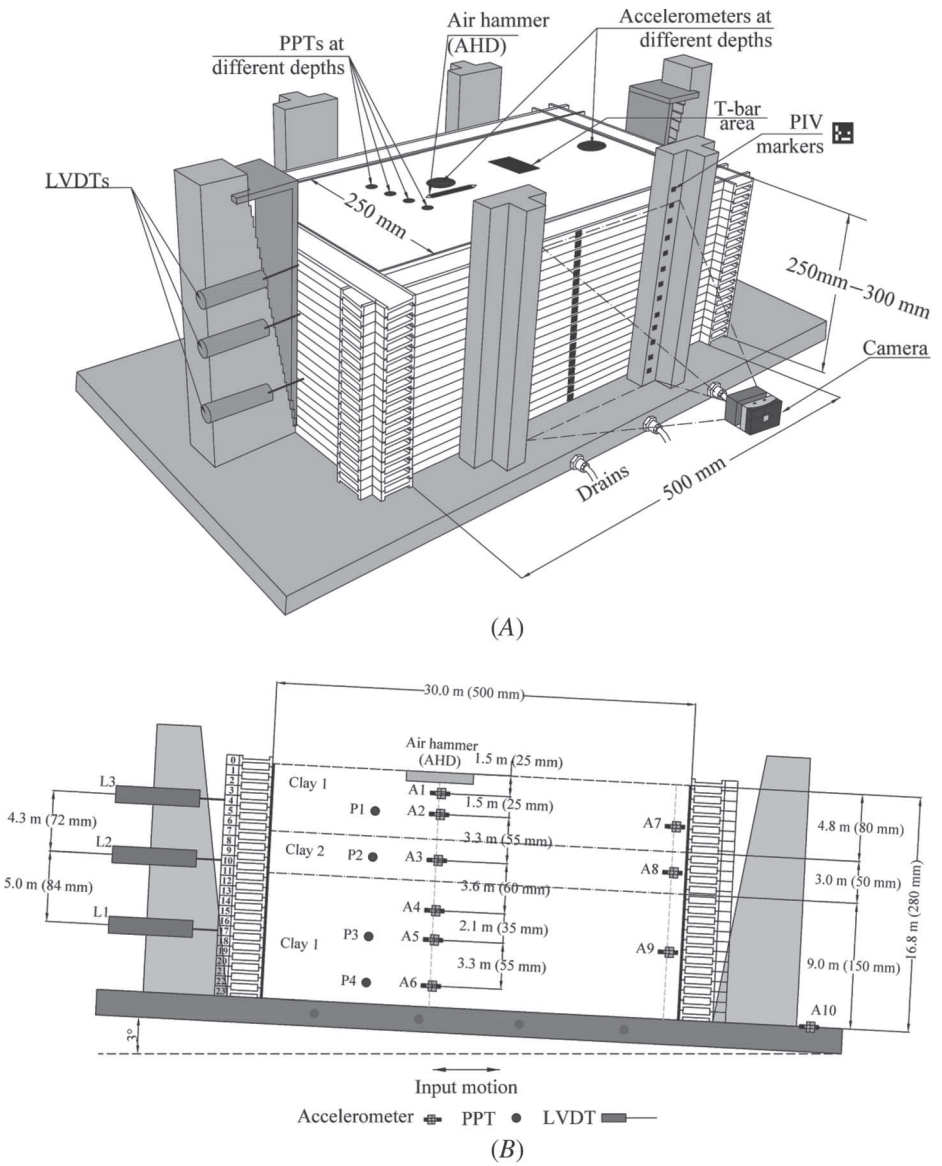

linked to the recording frame rate. For example, at a maximum resolution of 1,696 by 1,710 pixels, it is possible to record images at a frame rate of 523 Hz. For the centrifuge test reported here, a resolution of 1,504 by 1,050 pixels was employed, delivering a frame rate of 953 Hz.

The camera was triggered to record 15 % of the total frames prior to the trigger via an external signal, and the remaining percentage to record the earthquake itself. The recording time for the dynamic events in the centrifuge is of the order of a few seconds; for the current test, 1.4 s was sufficient to record a total of 1,354 photos (or frames) per earthquake.

Once the laminar container was assembled and the instruments were installed, ArUco markers (Garrido-Jurado et al. 2014) were glued to each lamina. Two sets of markers were used, the first set, which was labelled as

FIG. 3 View of the model in the servo-hydraulic actuator.

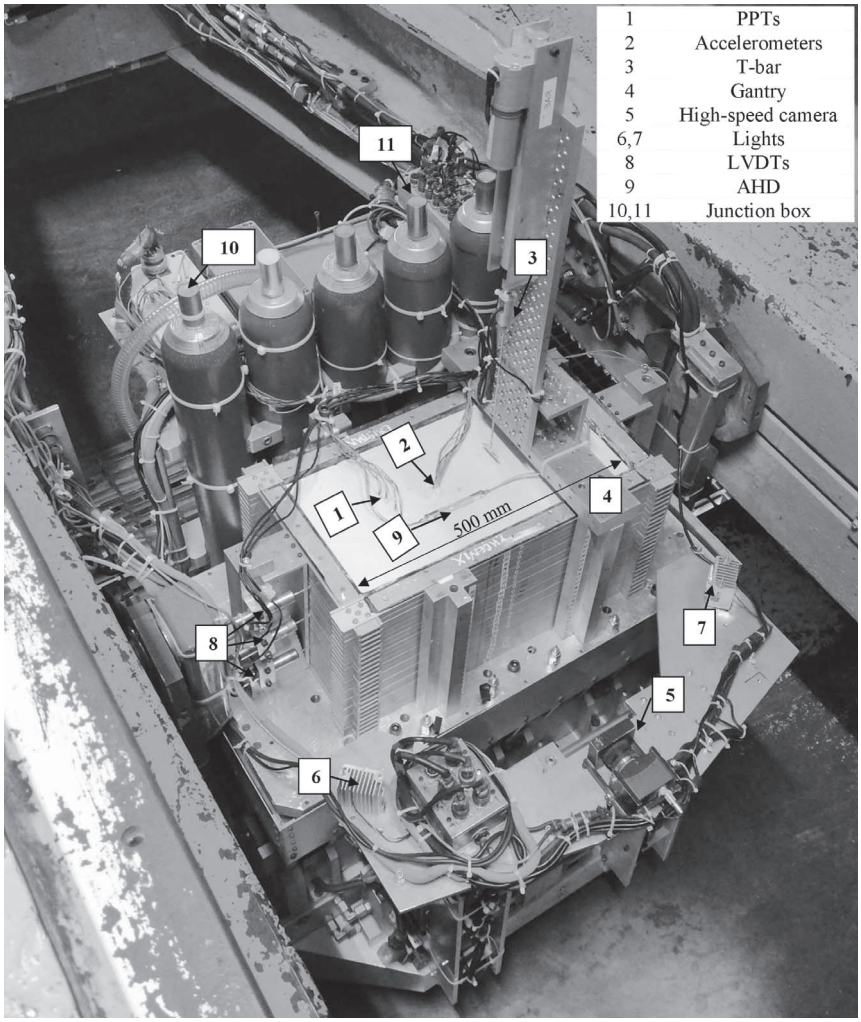

fixed column (fig. 4), was attached to the vertical, rigid columns that act as a boundary and support for the laminar container in the transverse direction. The displacement of the elements of the fixed column is related to the displacement of the shaking table, enabling tracking of the input motion. The second set of markers, labeled as displacement markers (fig. 4), was installed in the laminae of the container and used to track the displacement of the mass of soil at different depths. The three LVDTs installed on the side of the container were also used for comparison with and validation of the displacements tracked by the PIV method.

Blender is an open source software package for many purposes related to 2D and 3D animation (Hess 2010). Among its functionalities, there is a module for motion tracking that enables tracking of markers during a photo or video sequence. Options such as marker size, tracking area, correlation between matched and source image, and tracking methodologies are available. Blender uses a tracker with subpixel precision following a brute-force search with subpixel refinement. For the current test, a correlation coefficient of 0.95 and a tracking method called "location only," which looks for changes in translation of the markers, was used.

The tracking process begins by assigning initial coordinates to the markers to be tracked; in a frame the coordinates are in pixel units in the horizontal and vertical directions. This is performed by defining a pattern area

FIG. 4 Location and sets of markers (dimensions in model scale).

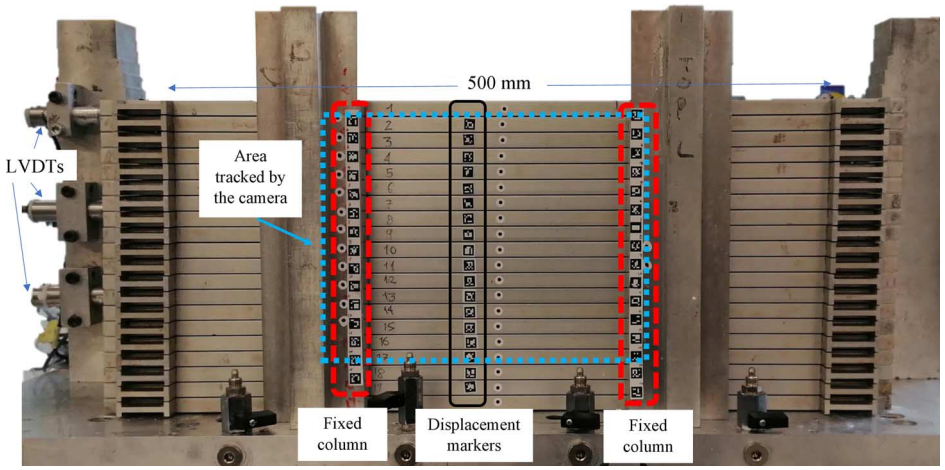

with a size equivalent to the dimensions of the marker. Next, a search area is established in which Blender will look for the position of the marker in the following frames. The definition of the pattern area and the search area is shown in **figure 5*A***. The search area was assigned to the markers based on their expected displacements during each earthquake motion. This area can be increased in case one of the markers moves beyond the defined range. After tracking the markers, the results were generated in terms of frame number, and the horizontal and vertical coordinates of each marker in pixels. Before the test, a checkerboard was placed in front of the camera in the same plane as the markers in order to associate real coordinates to the coordinates of the markers in the photos (1 pixel was equivalent to approximately 0.18 mm in model scale). **Figure 5*B*** shows the coordinate system for a photo in pixels and the corresponding equivalence in millimeters.

An example of the tracking of one marker is presented in **figure 6**. The coordinates of each marker (x_i, y_i) after being tracked are in units of pixels and presented frame by frame with a total of 1,354 frames tracked in a period of 1.4 s (frame rate 953 Hz) as previously discussed. According to the camera settings and position, an area of 1,504 by 1,050 pixels covering 15 out of 23 laminations of the model container. The scaling between pixel units

FIG. 5 Tracking of markers: (*A*) screenshot of Blender, pattern, and search area for the markers; (*B*) photo in pixels and scaled in millimeters.

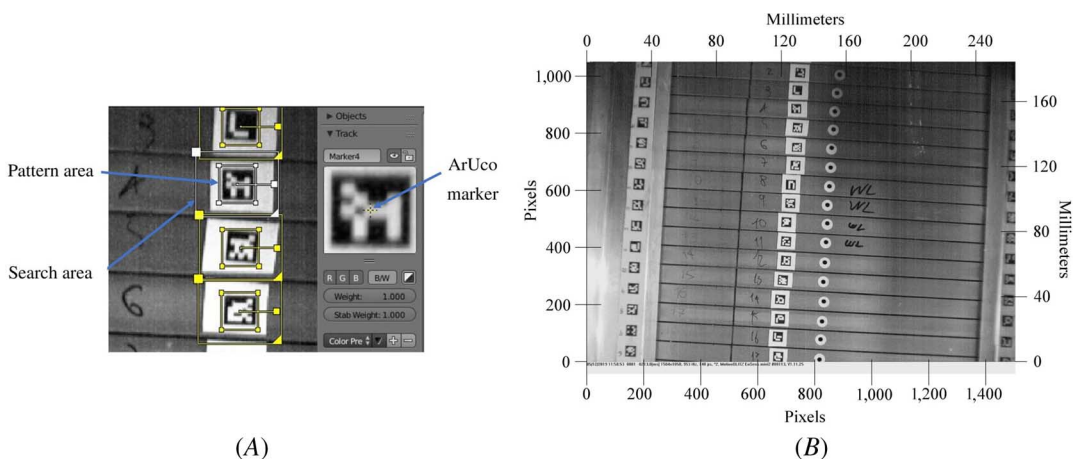

FIG. 6 Example of tracking of a marker (model units in parenthesis).

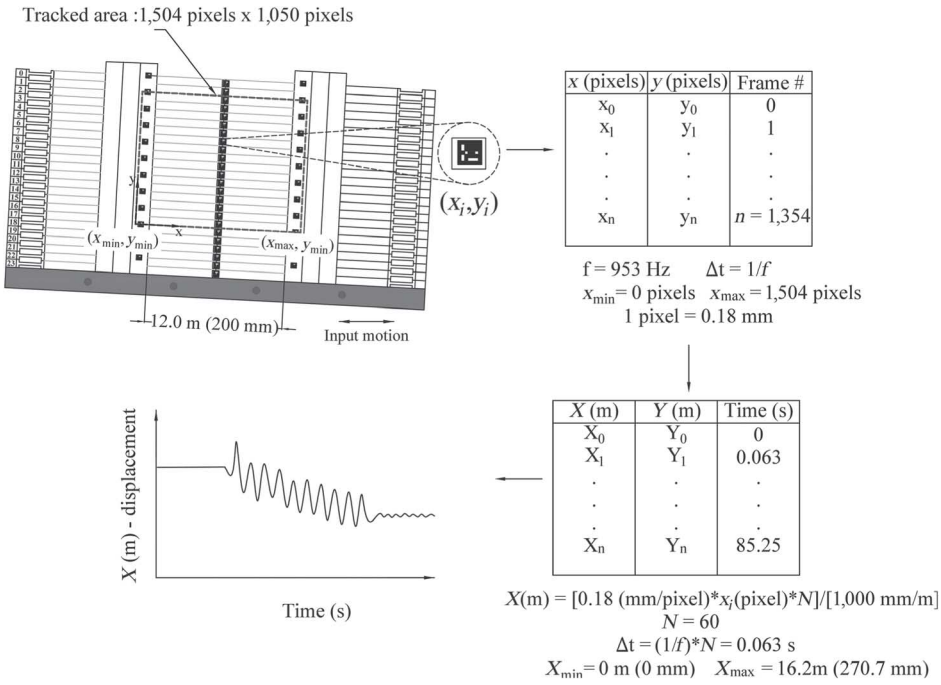

and distance units is performed using a known length employing a checkerboard, as mentioned above, then a relationship of a 1-pixel equivalent to approximately 0.18 mm in model scale was obtained. Finally, each coordinate of the marker is expressed in prototype units (X_i,Y_i), the time step is obtained from the sampling frequency, and the variation of the horizontal displacement is plotted with time. Considering the displacements occur in the downslope orientation, there was no variation of displacements in the y (vertical) direction (also for the boundary condition imposed by the laminar container); however, the methodology can also be applied to problems in which it is necessary to track displacements in this direction.

Experimental Program and Testing

To simulate the gentle slope inclination, the model was tilted by 3° using wedges placed along the base of the model. The swing up of the model consisted of increments of 10 g until reaching the acceleration level for the test (60 g). The bottom drains of the model container were closed during the centrifuge test. Air hammer tests (AHTs) were performed at the different stages of the spinning up of the model and between the shaking events to estimate the shear wave velocities within the soil profile in flight. Accelerometers were used to measure the arrival times generated by the air hammer placed on top of the clay (Ghosh and Madabhushi 2002). Once the target acceleration level was achieved, the model was maintained inflight for 40 min before the application of the earthquakes to increase the total stresses and redistribute the pore pressures and effective vertical stresses; a similar methodology was adopted by Garala, Madabhushi, and Di Laora (forthcoming). In the present test program, all centrifuge tests had a similar inflight time before the application of the earthquakes, and all showed similar undrained strength profiles. The following stage consisted of a T-bar penetrometer test (Stewart and Randolph 1991) and an additional AHT. The T-bar used was 40 mm wide with a 4 mm diameter and was pushed into the clay at a rate of approximately 2 mm/s. The normalized penetration rate, V, is (after Finnie and Randolph 1994).

FIG. 7 Clay model properties: (*A*) stress history, (*B*) undrained shear strength profiles, and (*C*) shear wave velocity profile.

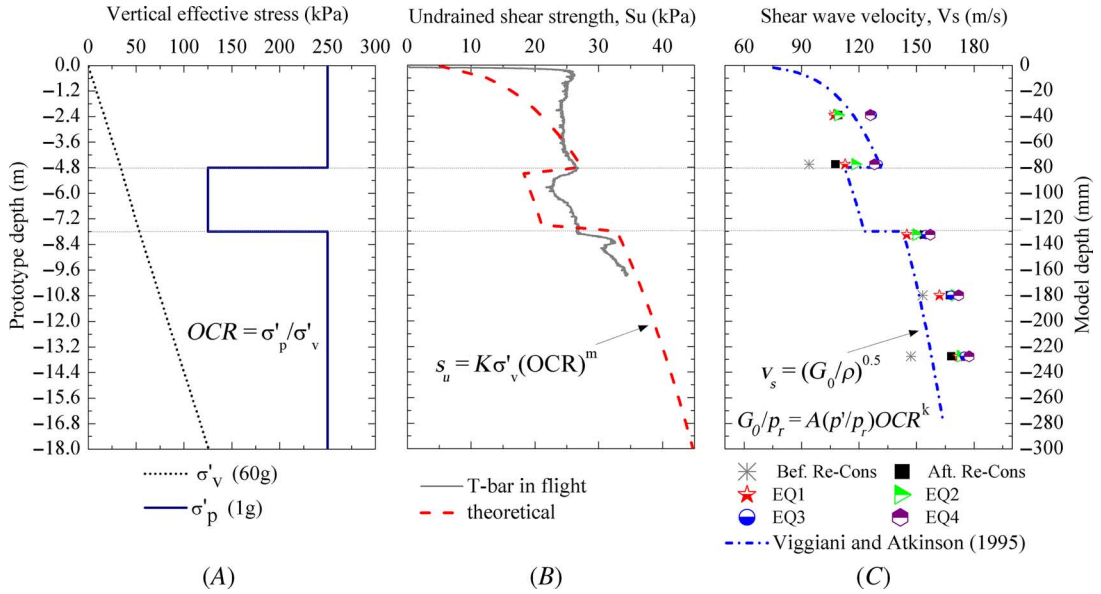

$$V = \frac{\nu D}{c_\nu} \tag{1}$$

where:

v = penetration velocity of the T-bar, 2 mm/s;
D = diameter of the T-bar, 4 mm; and
c_v = coefficient of consolidation of the kaolin, 4.29 mm^2/min (0.07 mm^2/s) (Chow et al. 2020).

For clays, normalized velocities (V) greater than 10 are likely to be undrained (Oliveira et al. 2011; Randolph and Gourvenec 2011), for the current test $V = 114$, therefore ensuring that the T-bar penetrometer test was performed at an undrained rate.

The results of the in-flight characterization of the clay are presented in **figure 7** in terms of effective vertical stresses applied to the model, undrained strength profiles, and shear wave velocity profiles.

UNDRAINED SHEAR STRENGTH PROFILE

The measured undrained shear strength (s_u) profile is presented together with an estimate derived from the well-known stress history relationship (equation (2); Wroth 1984):

$$s_u = K\sigma'_\nu (OCR)^m \tag{2}$$

where:

K = normalized strength parameter;
$\sigma'_\nu = (\gamma_{sat} - \gamma_{water})^* Z$ = effective vertical stress in kPa;
$OCR = \sigma'_p/\sigma'_v$ = overconsolidation ratio;
m = power constant in the equation;
γ_{sat} = saturated unit weight – 16.9 kN/m^3 (top/bottom layers); 16.4 kN/m^3 (weak layer); and
σ'_p = pre-consolidation pressure of the layer – 250 kPa and 125 kPa.

Values of the K and m constants have been reported by several authors (Almeida 1984; Springman 1989; Sharma and Bolton 1996). The theoretical curve was calculated based on the parameters presented by Zhang,

White, and Randolph (2011) ($K = 0.23$, $m = 0.62$). The overconsolidation ratio (OCR) was calculated as the ratio of the maximum past effective consolidation stresses ($\sigma'_p = 250$ kPa and $\sigma'_p = 125$ kPa) and the effective vertical stress in flight (σ'_v). The distribution of the effective vertical stresses and pre-consolidation pressures used for the calculation of the OCR are presented in **figure 7A**. A reasonably good agreement is evident between the experimental and theoretical curves (**fig. 7B**) exhibiting an increase with depth and a reduction in the weaker layer in which a lower pre-consolidation pressure has been applied. The observed contrast of s_u between the weak layer and the neighbouring layers of around 20 % lower strength is in accordance with in-situ measured s_u profiles (Soriano et al., n.d.). There are higher measured values of s_u on top of the clay (between 0 and 3.6 m) compared with the theoretical curve. This may be due to partial drying of the clay during the swing up and the fact that no surficial water was added to the model in order to avoid sloshing during the earthquake experiments.

SHEAR WAVE VELOCITY PROFILE

The shear wave velocities measured by the air hammer were compared with a well-known small-strain stiffness correlation (equation (3)) based on the Viggiani and Atkinson (1995) equation:

$$\frac{G_0}{p_r} = A\left(\frac{p'}{p_r}\right)^M OCR^k \tag{3}$$

where:

G_0 = initial shear modulus in kPa;
p' = mean effective stress in kPa;
p_r = reference pressure equivalent to 1 kPa;
OCR = overconsolidation ratio;
A = correlated parameter;
k = correlated parameter; and
M = correlated parameter.

The selection of the correlated parameters (A, k, M) was based on the PI of the clay (PI = 33 %). The relationship between the PI and the parameters is presented in Viggiani and Atkinson (1995); for the current research, $A = 950$, $k = 0.24$, and $M = 0.8$. The shear wave velocity (V_s) was calculated in terms of the initial shear modulus (G_0) and the soil density (ρ) expressed as the total unit weight divided by gravity (equation (4)):

$$V_S = \sqrt{\frac{G_o}{\rho}} \tag{4}$$

The estimation of the shear wave velocities was based on the travel times between the signals captured by the accelerometers (A1 to A6 in **fig. 2B**) when the shear waves produced by the air hammer passed through them. To ensure the precision in the recording of the arrival times, it is necessary to have relatively high sampling frequencies. For the current test, a sampling frequency of 30 kHz was used for the AHTs. Some uncertainties are involved during AHTs (McCullough et al. 2007), such as the location of the instruments, given the permanent deformations that occur during testing (due to swing up and application of earthquakes); therefore, the shear waves may reflect some error. Despite the uncertainties of the AHT, the measured values of the shear wave velocities appear to be in good agreement with the empirical formula (**fig. 7C**). A slight increase in the measured shear wave velocities can also be observed, as the different stages of the test occurred with the lowest values before the reconsolidation of the clay and the highest values after the application of the earthquake EQ4. This implies that there is a hardening of the clay under cyclic loading as the shaking progresses. The fundamental period of the soil profile was 0.5 s. It was estimated by weighted average of shear wave velocity for multiple layer soil using the values from the correlated curve obtained from equation (4), dividing the profile in sublayers of 0.10 m, and using the following equation (equation (5)):

$$T = \frac{4H^2}{\sum_{i=1}^{n} V_i H_i} \tag{5}$$

where:

T = fundamental period (s);
H = thickness of the soil profile (m);
V_i = shear wave velocity of the corresponding layer (m/s); and
H_i = thickness of the sublayer (m).

SHAKING EVENTS

The model was subjected to four earthquakes, three consisting of sinusoidal motions with a driven frequency of 1 Hz and the other, a scaled real motion (Kobe earthquake, 1995). During the application of the earthquakes, the instrument data were recorded at a sampling frequency of 6 kHz. Table 1 shows the salient characteristics of the earthquakes applied to the model in prototype and model scale. The sequence of the input motions was defined in

TABLE 1
Model earthquakes

		Frequency, Hz		Duration, s		Peak Base Acceleration, g	
Input Motion	Type	Prot.	Model	Prot.	Model	Prot.	Model
EQ1	Sinusoidal	1	60	10	0.17	0.06	3.6
EQ2	Kobe (scaled)	1.4–2.4	84.0–142.8	4.3	0.07	0.18	10.8
EQ3	Sinusoidal	1	60	10	0.17	0.18	10.8
EQ4	Sinusoidal	1	60	10	0.17	0.37	22.2

Note: Prot. = Prototype.

FIG. 8
Input motions in prototype scale.

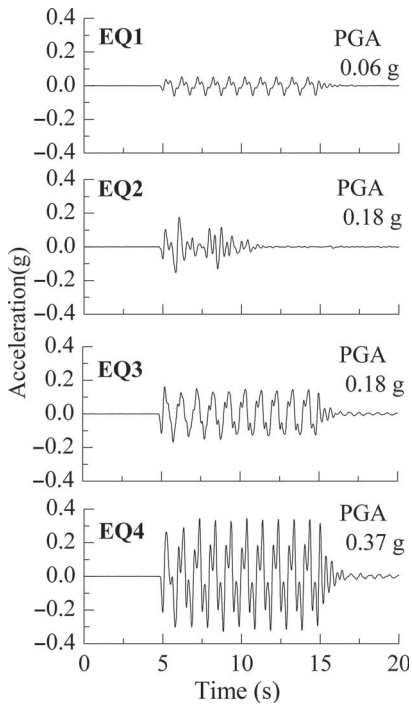

terms of increasing amplitude. Figure 8 presents the acceleration-time histories recorded at the base of the model (accelerometer A10 in fig. 2B) or input motions presented in terms of prototype scale.

Test Results

DISPLACEMENT-TIME HISTORIES

The displacement time histories recorded by the LVDTs and calculated by PIV are plotted together with the corresponding input motions in figure 9B and 9C. The location of the LVDTs and the corresponding markers used for comparison of the displacement-time histories is presented in figure 9A. For brevity, only the results of earthquakes EQ2 (real scaled) and EQ3 (sinusoidal) are presented in prototype scale. The results show excellent agreement (both series overlap) between the data measured by the LVDTs and the displacements calculated by the PIV methodology incorporated in the Blender software. This validates the use of the ArUco markers for tracking the motions of each of the individual laminae, which is not possible using LVDTs because of their size.

ACCELERATION TIME HISTORIES

The acceleration time histories and fast Fourier transforms (FFTs) at different depths for earthquakes EQ2 and EQ3 are presented in figure 10. The results are presented in prototype scale. In addition, from the displacement time histories obtained from the PIV analysis, approximate accelerations at the depths of the corresponding accelerometers were calculated using double differentiation (fig. 10A and 10C). The raw data from the accelerometers were filtered using a fourth-order Butterworth-type filter with a bandpass between 5 and 350 Hz in terms of model scale. The selected range of frequencies was defined to remove the low frequencies that produce a drift in the accelerometer signal and the high frequencies associated with electrical noise. The corresponding FFTs

FIG. 9 Displacement-time histories: (*A*) location of the LVDTs and markers used for comparison, (*B*) horizontal displacements during earthquake EQ2, and (*C*) horizontal displacements during earthquake EQ3.

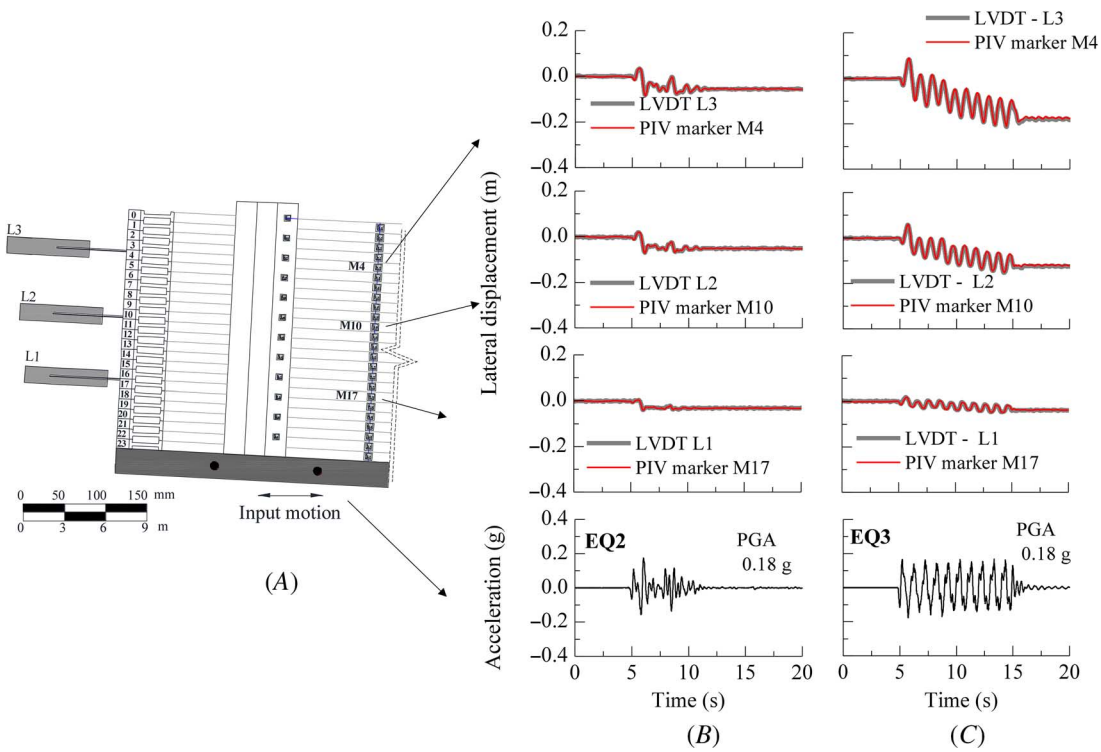

FIG. 10 Propagation of input motions along the clay: (*A*) earthquake EQ 2 accelerations, (*B*) earthquake EQ2 Fourier spectra, (*C*) earthquake EQ3 accelerations, and (*D*) earthquake EQ3 Fourier spectra.

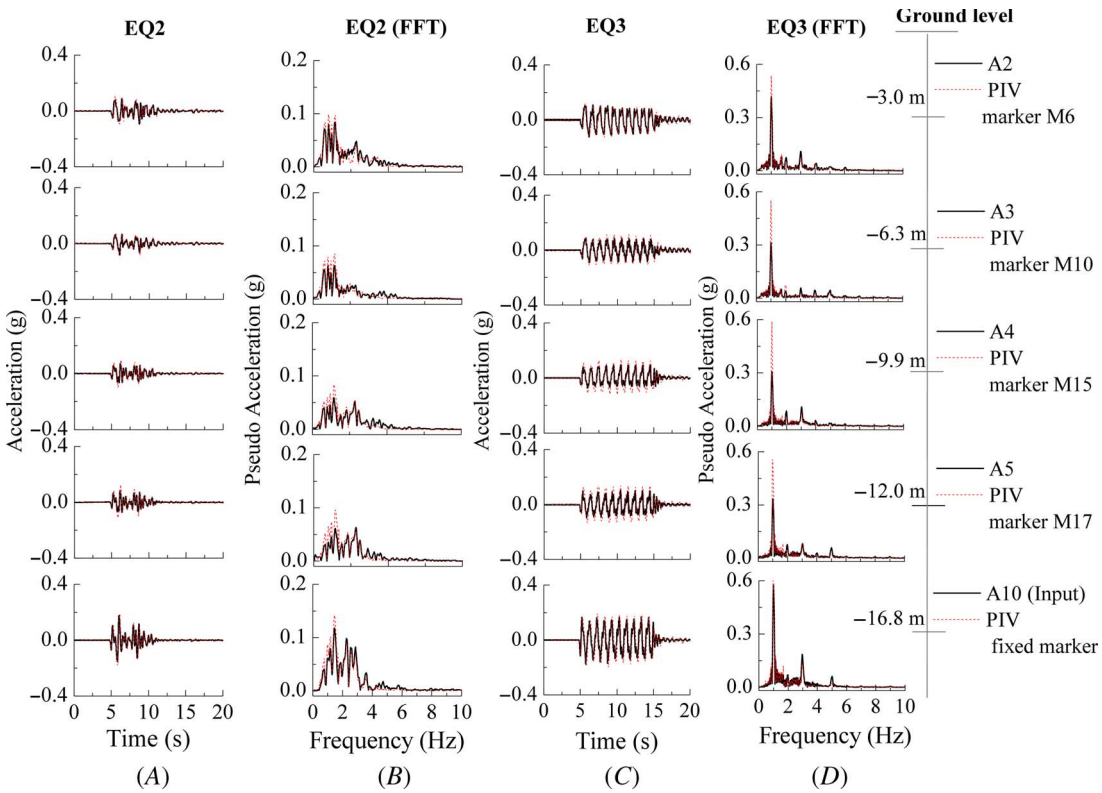

of the signals at different depths are presented in **figure 10*B*** and **10*D***. The FFT results displayed in **figure 10*D*** indicate that although earthquake EQ3 was applied as a single frequency (1 Hz) sine wave as stated in **Table 1**, the recorded signal is not totally harmonic and other features can be seen in the frequency domain representation. According to Brennan, Thusyanthan, and Madabhushi (2005), the load applied by a centrifuge earthquake actuator and transferred to the laminar container is not necessarily single frequency. The observed higher harmonics reflect part of the vibration of the shaker and transmitted to the laminar box and are therefore real loading components and cannot be considered as noise. This behavior was also observed in the PIV results where the main frequency of the input motions and the higher frequencies were also captured.

PEAK GROUND ACCELERATIONS AND HORIZONTAL DISPLACEMENTS

The slope response was evaluated by means of maximum displacement profile, peak ground acceleration (PGA) profile, 5 %-damped accelerations at the base and near the surface (1.5-m depth), and the ratios of the response spectra. **Figure 11** presents the peak lateral displacements and PGA profiles obtained after the application of the earthquakes to the model. It must be pointed out that the displacements were plotted for each earthquake by resetting the displacements to zero prior to that earthquake and assuming that the displacement at the base of the slope is zero (net displacements). These displacements are extrapolated in **figure 11*A*** as dashed lines below a 12-m depth. The values were obtained from the PIV analysis of the markers installed on the laminae (markers M2 to M17 in **fig. 11**) of the container and previously validated with the LVDT measurements (see **fig. 9**). **Figure 11*B*** shows the PGA variation with depth, with values obtained from two sources: the continuous profile from the PIV using the second derivative of the displacements at each marker depth and the individual points

FIG. 11 Slope response profiles: (*A*) maximum displacements and (*B*) PGA.

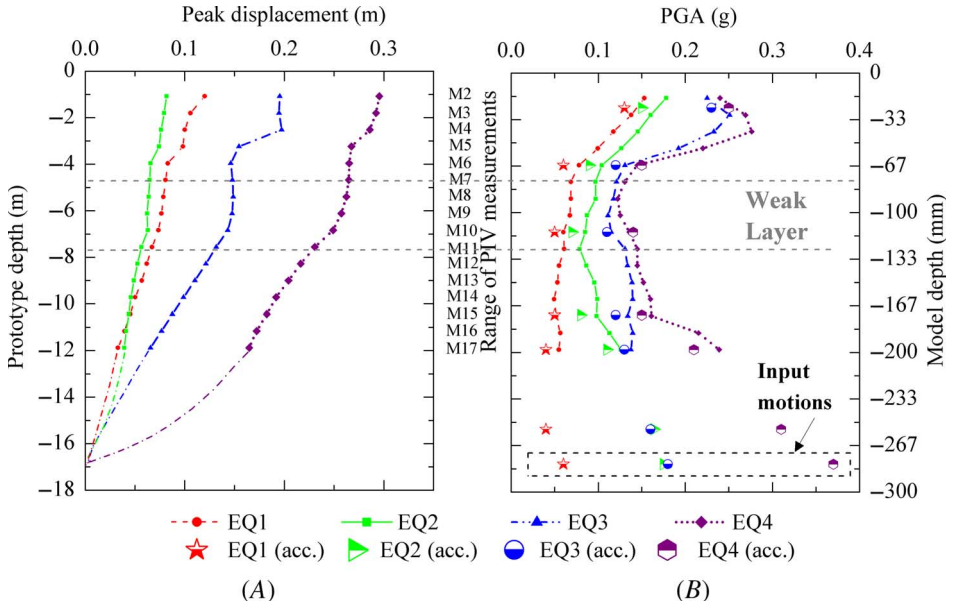

FIG. 12 (*A*) Acceleration response spectra and (*B*) response spectra ratio.

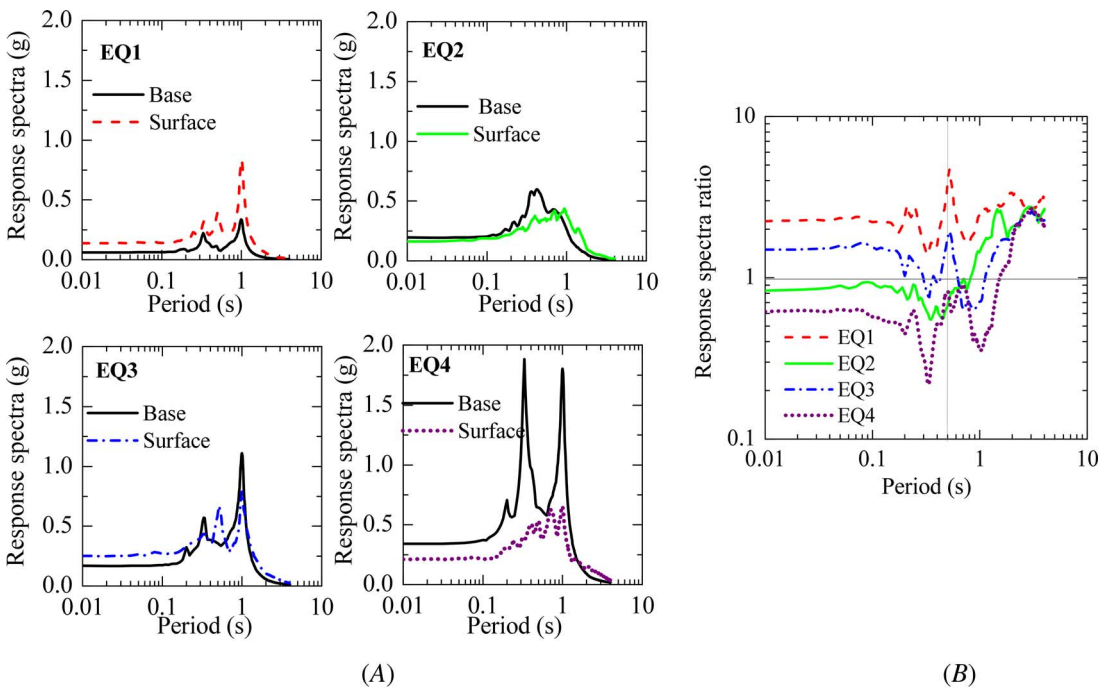

(identified as "acc.") from the accelerometer data. The results of the PGA profile show a good agreement between the approximation obtained by the PIV calculations and the values measured with the accelerometers. However, a small overestimation of the PGA in the values obtained by the PIV was observed when compared with the accelerometer data. This overestimation could be attributed to the fact that the PIV in the current test

FIG. 13

(*A*) Clay model after centrifuge test (model scale in parentheses) and (*B*) transversal section and contact between layers.

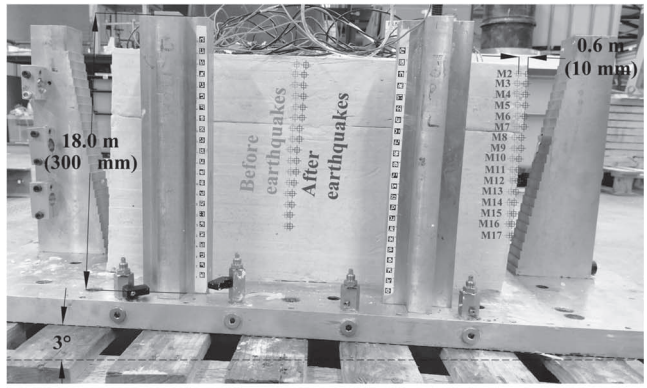

(*A*)

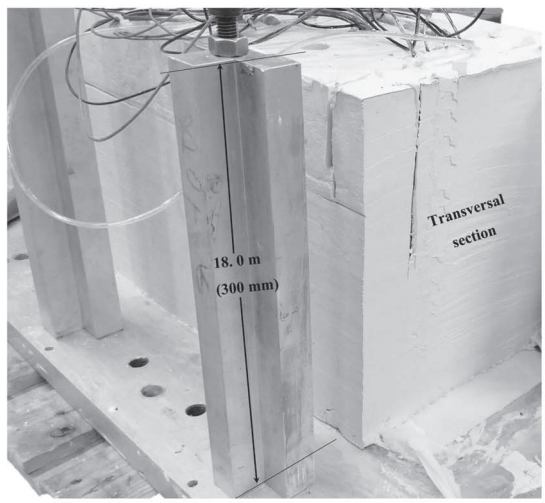

(*B*)

was intended to measure the displacements during the application of the earthquakes, and the accelerations from this method were obtained by double differentiation; therefore, it is not a direct measurement of the acceleration. Overall, the net displacements show an increase from the bottom to the top, as the earthquake amplitude increased with values ranging between 0.08 and 0.3 m at the top of the slope in terms of prototype scale. The PGA profiles for earthquakes EQ2, EQ3, and EQ4 exhibit attenuation at depths between 3 and 10 m in the soil profile.

Figure 12*A* shows the acceleration response spectra of the earthquakes applied to the model at the base and at a depth near the surface (−1.5 m) with a damping ratio of 5 %, and figure 12*B* presents the ratio of the response spectra curves. The response spectra ratios exhibit amplifications at the natural period of the soil profile (0.5 s) during earthquakes EQ1 and EQ3 corresponding to sinusoidal loadings, indicating the local site effects on the input motion. For EQ2, the response spectra ratio remained in a range close to 1 for the periods below 1 s, followed by amplification at periods greater than 1 s. For the largest amplitude earthquake (EQ4), the peak in the response spectra ratio shifted to a value of 0.7 s followed by an attenuation until 1 s and then a gradual increase, reaching values larger than 1. This shift in the peak of the response spectra ratio for earthquake EQ4 may be explained by nonlinear effects resulting from the reduction in the stiffness of the soil and the increase in damping as the soil softens.

Although strength mobilization may occur during the swing up of the model, a snapshot of the strength of the clay at the moment before the application of the shaking events was captured by means of the in-flight characterization tests (T-bar and air hammer). Further improvements can be implemented to control the lateral displacements during the swing up, using lateral actuators that laterally support the laminar container with the clay through the swing up process and are released prior to the application of the earthquakes. For the calibration of a numerical model, the selection of the strength parameters must consider the monotonic strengths and the cyclic strengths given by the strain rates applied in centrifuge tests. Strain rate effects significantly increase the strength and stiffness in clays (Afacan et al. 2019; Sathialingam and Kutter 1989).

POST-TEST INVESTIGATIONS

A photograph of the model after the test and an overlay of the location of the markers tracked by the camera is shown in **figure 13*A***. An accumulated displacement is evident on top of the clay at about 10 mm (model scale). An interface line between the clay layers was visible at the periphery of the sample. Thus, to determine the continuity and contact between the layers, a section in the transverse direction was checked. No evidence of discontinuity between the layers was apparent in those transverse sections; therefore, the model soil profile was laterally uniform (**fig. 13*B***), indicating a successful sample preparation process.

Conclusions and Recommendations for Similar Testing Programs

The centrifuge test in this study was performed to develop a model preparation technique for simulating the dynamic behavior of a gentle layered slope in soft clay. The model was subjected to a series of dynamic motions to investigate the displacement and acceleration behaviors. The main observations from the centrifuge test follow:

- The proposed model preparation technique enabled the simulation of a three-layer soil profile in clay, with a strength contrast between layers achieved by applying different consolidation pressures during the sample preparation process.
- The PIV analysis was used to track the displacements of the model at the different stages of the centrifuge test with particular focus on the application of the dynamic motions. The displacements from the PIV calculations were in good agreement with those measured by the LVDTs, confirming that a similar setup could be applied in comparable testing programs involving the use of laminar containers.
- Measured soil properties for undrained shear strength and shear wave velocity were in reasonable agreement with the empirical predictions.
- The acceleration data at different depths were obtained by direct measurements from the accelerometers and approximated by double differentiation of the PIV displacements. The results were compared in terms of the time histories and the FFT of the signals. Additional frequencies were observed on the sinusoidal motions attributable to the higher vibration modes of the shaker and were transmitted to the laminar container.
- With the validated PIV results, a continuous displacement profile after the applied earthquakes was calculated. The PGA profiles were obtained from the maximum accelerations measured by the accelerometers and from the double derivative of the displacements calculated from the PIV analyses. The results are complementary and show good agreement and could be used for direct comparison with computational analyses.
- The spectral analysis showed amplifications at periods corresponding to the fundamental period of the soil profile during earthquakes EQ2 and EQ3. A shift in the period occurred during the largest amplitude earthquake (EQ4), indicating a nonlinear behavior of the slope profile.
- In addition to the monotonic strengths, given the strain rates applied in dynamic centrifuge tests, cyclic strengths should also be considered for the calibration of numerical models of the problem studied.

The results from the centrifuge test provided useful insight into preparation of layered clay-profile models using a laminar container to assess lateral spreading problems. The results can be used for calibration of numerical

models and for performing comparisons with existing methods for the calculation of dynamic responses (i.e., Newmark's method).

ACKNOWLEDGMENTS

The authors thank the staff of the Schofield Centre at the University of Cambridge for carrying out the testing program presented in this work, as well as Dr. Zheng Li and Dr. Samuel Tarazona for their insightful recommendations. The work described in this article is part of a Cooperation Agreement, between PETROBRAS and the Federal University of Rio de Janeiro, to develop a research project titled 'Seismic Centrifuge Modelling of Gentle Slopes' (Contractual Instrument 2017/00259-5). This study was also partially funded by the Rio de Janeiro State Research Foundation (FAPERJ) and the National Institute of Science and Technology – REAGEO.

References

Acosta, E., S. Tibana, M. S. S. Almeida, and F. Saboya. 2017. "Centrifuge Modeling of Hydroplaning in Submarine Slopes." *Ocean Engineering* 129, no. 1 (January): 451–458. https://doi.org/10.1016/j.oceaneng.2016.10.047

Afacan, K. B., S. J. Brandenberg, and P. J. Stewart. 2014. "Centrifuge Modeling Studies of Site Response in Soft Clay over Wide Strain Range." *Journal of Geotechnical and Geoenvironmental Engineering* 140, no. 2 (February): 1–13. https://doi.org/10.1061/(ASCE)GT.1943-5606.0001014

Afacan, K. B., S. Yniesta, A. Shafiee, J. Stewart, and S. Brandenberg. 2019. "Total Stress Analysis of Soft Clay Ground Response in Centrifuge Models." *Journal of Geotechnical and Governamentaliza Engineering* 145, no. 10 (October): 04019061. https://doi.org/10.1061/(ASCE)GT.1943-5606.0002115

Almeida, M. S. S. "Stage Constructed Embankments on Soft Clays." PhD diss., Cambridge University, 1984.

Biscontin, G. and J. Pestana. 2006. "Factors Affecting Seismic Response of Submarine Slopes." *Natural Hazards and Earth System Science* 6, no. 1 (January): 97–107. https://doi.org/10.5194/nhess-6-97-2006

Biscontin, G., J. M. Pestana, and F. Nadim. 2004. "Seismic Triggering of Submarine Slides in Soft Cohesive Soil Deposits." *Marine Geology* 203, nos. 3–4 (January): 341–354. https://doi.org/10.1016/S0025-3227(03)00314-1

Borges, R. G., M. Assumpção, M. C. F. Almeida, and M. S. S. Almeida. 2020. "Seismicity and Seismic Hazard in the Continental Margin of Southeastern Brazil." *Journal of Seismology* 242 (July): 1205–1224. https://doi.org/10.1007/s10950-020-09941-4

Brennan, A. J., S. P. G. Madabhushi, and P. Cooper. n.d. "Dynamic Centrifuge Testing of Suction Caissons in Soft Clay." Paper presented at the Sixth International Conference on Physical Modelling in Geotechnics, Hong Kong, August 4–6, 2006.

Brennan, A. J., S. P. G. Madabhushi, and N. E. Houghton. n.d. "Comparing Laminar and Equivalent Shear Beam (ESB) Containers for Dynamic Centrifuge Modeling." Paper presented at the Sixth International Conference on Physical Modelling in Geotechnics, Hong Kong, August 4–6, 2006.

Brennan, A. J., N. I. Thusyanthan, and S. P. G. Madabhushi. 2005. "Evaluation of Shear Modulus and Damping in Dynamic Centrifuge Tests." *Journal of Geotechnical and Geoenvironmental Engineering* 131, no. 12 (December): 1488–1498. https://doi.org/10.1061/(ASCE)1090-0241(2005)131:12(1488)

Bryn, P., K. Berg, C. F. Forsberg, A. Solheim, and T. J. Kvalstad. 2005a. "Explaining the Storegga Slide." *Marine and Petroleum Geology* 22, nos. 1–2 (January/February): 11–19. https://doi.org/10.1016/j.marpetgeo.2004.12.003

Bryn, P., K. Berg, M. S. Stoker, H. Haflidason, and A. Solheim. 2005b. "Contourites and Their Relevance for Mass Wasting along the Mid-Norwegian Margin." *Marine and Petroleum Geology* 22, nos. 1–2 (January/February): 85–96. https://doi.org/10.1016/j.marpetgeo.2004.10.012

Chow, J. K., Y. Wang, H. L. Lui, and E. Huang. 2020. "Determination of Consolidation Parameters Based on the Excess Pore Water Pressure Measurement Using a Newly Developed U-Oedometer." *Acta Geotechnica* 15 (February): 2665–2680. https://doi.org/10.1007/s11440-020-00914-y

De Sanctis, L., R. Di Laora, T. K. Garala, S. P. G. Madabhushi, G. Viggiani, and P. Fargnoli. 2021. "Centrifuge Modelling of the Behaviour of Pile Groups under Vertical Eccentric Load." *Soils and Foundations* 61, no. 2 (April): 465–479. https://doi.org/10.1016/j.sandf.2021.01.006

Dey, R., B. Hawlader, R. Phillips, and K. Soga. 2016. "Modeling of Large Deformation Behaviour of Marine Sensitive Clays and Its Application to Submarine Slope Stability Analysis." *Canadian Geotechnical Journal* 53, no. 7 (July): 1138–1155. https://doi.org/10.1139/cgj-2015-0176

Elgamal, A. W., M. Zeghal, V. Taboada, and R. Dobry. 1996. "Analysis of Site Liquefaction and Lateral Spreading Using Centrifuge Testing Records." *Soils and Foundations* 36, no. 2 (June): 111–121. https://doi.org/10.3208/sandf.36.2_111

Fagundes, D. F., K. I. Rammah, M. S. S. Almeida, J. Pequeno, J. R. M. S. Oliveira, and R. G. Borges. 2012. "Strength Behaviour Analysis of an Offshore Brazilian Marine Clay." In *Proceedings of the ASME 2012 31st International Conference on Ocean, Offshore and Arctic Engineering*, OMAE2012-83008. New York: American Society of Mechanical Engineers.

Finnie, I. M. S. and M. F. Randolph. 1994. "Punch-Through and Liquefaction Induced Failure on Shallow Foundations on Calcareous Sediments." In *Seventh International Conference on the Behaviour of Offshore Structures*, 217–230. Boston, MA: Pergamon.

Garala, T. K. and S. P. G. Madabhushi. 2019. "Seismic Behaviour of Soft Clay and Its Influence on the Response of Friction Pile Foundations." *Bulletin of Earthquake Engineering* 17 (November): 1919–1939. https://doi.org/10.1007/s10518-018-0508-4

Garala, T. K., S. P. G. Madabhushi, and R. Di Laora. Forthcoming. "Experimental Investigation of Kinematic Pile Bending in Layered Soils Using Dynamic Centrifuge Modelling." *Geotechnique*. Published ahead of print, December 14, 2020. https://doi.org/10.1680/jgeot.19.p.185

García-Torres, S. and S. P. G. Madabhushi. 2019. "Performance of Vertical Drains in Liquefaction Mitigation under Structures." *Bulletin of Earthquake Engineering* 17 (September): 5849–5866. https://doi.org/10.1007/s10518-019-00717-x

Garrido-Jurado, S., R. Muñoz-Salinas, F. Madrid-Cuevas, and M. Marín-Jiménez. 2014. "Automatic Generation and Detection of Highly Reliable Fiducial Markers under Occlusion." *Pattern Recognition* 47, no. 6 (June): 2280–2292. https://doi.org/10.1016/j.patcog.2014.01.005

Ghosh, B. and S. P. G. Madabhushi. 2002. "An Efficient Tool for Measuring Shear Wave Velocity in the Centrifuge." In *Physical Modelling in Geotechnics—ICPMG '02*, edited by P. Guo, R. Phillips, and R. Popescu, 119–124. Boca Raton, FL: CRC Press.

Haflidason, H., H. P. Sejrup, I. M. Berstad, A. Nygard, T. Richter, R. Lien, and K. Berg. 2003. "A Weak Layer Feature on the Northern Storegga Slide Escarpment." In *European Margin Sediment Dynamics*, edited by J. Mienert and P. P. E. Weaver, 55–62. Berlin, Germany: Springer.

Haigh, S. K., S. P. G. Madabhushi, K. Soga, Y. Taji, and Y. Shamoto. n.d. "Lateral Spreading during Centrifuge Model Earthquakes." Paper presented at ISRM International Symposium, Melbourne, Australia, November 19–24, 2000.

Hess, R. 2010. *Blender Foundations: The Essential Guide to Learning Blender 2.6*. Waltham, MA: Focal Press.

Hotta, M. M., M. S. S. Almeida, D. T. Pelissaro, J. R. M. S. Oliveira, S. Tibana, and R. G. Borges. 2020. "Centrifuge Tests for Evaluation of Submarine-Mudflow Hydroplaning and Turbidity Currents." *International Journal of Physical Modelling in Geotechnics* 20, no. 4 (July): 239–253. https://doi.org/10.1680/jphmg.18.00081

Hühnerbach, V. and D. G. Masson. 2004. "Landslides in the North Atlantic and Its Adjacent Seas: An Analysis of Their Morphology, Setting and Behavior." *Marine Geology* 213, nos. 1–4 (December): 343–362. https://doi.org/10.1016/j.margeo.2004.10.013

Kim, S. H. "Model Testing and Analysis of Interactions between Tunnels in Clay." PhD diss., University of Oxford, 1996.

Knappett, J. A. "Piled Foundations in Liquefiable Soils: Accounting for Axial Loads." PhD diss., Cambridge University, 2006.

Kowsmann, R. O, A. C. Lima, and M. A. Vicalvi. 2016. "Features Indicating Geological Instability in the Continental Slope and São Paulo Plateau." In *Geology and Geomorphology. Regional Environmental Characterization of the Campos Basin, Southwest Atlantic*, edited by R. O. Kowsmann, 71–97. Amsterdam, the Netherlands: Elsevier. https://doi.org/10.1016/B978-85-352-8444-7.50012-3

Lanzano, G., E. Bilotta, G. Russo, F. Silvestri, and S. P. G. Madabhushi. 2012. "Centrifuge Modeling of Seismic Loading on Tunnels in Sand." *Geotechnical Testing Journal* 35, no. 6 (November): 854–869. https://doi.org/10.1520/GTJ104348

Lau, B. H. "Cyclic Behaviour of Monopile Foundations for Offshore Wind Turbines in Clay." PhD diss., University of Cambridge, 2015.

Locat, J. and H. Lee. 2009. "Submarine Mass Movements and Their Consequences: An Overview." In *Landslides and Disaster Risk Reduction*, edited by K. Sassa and P. Canuti, 115–142. Berlin, Germany: Springer. https://doi.org/10.1007/978-3-540-69970-5_6

Madabhushi, S. P. G. 2014. *Centrifuge Modelling for Civil Engineers*. Boca Raton, FL: CRC Press.

Madabhushi, S. P. G., S. K. Haigh, N. E. Houghton, and E. Gould. 2012. "Development of a Servo-Hydraulic Earthquake Actuator for the Cambridge Turner Beam Centrifuge." *International Journal of Physical Modelling in Geotechnics* 12, no. 2 (June): 77–88. https://doi.org/10.1680/ijpmg.11.00013

McCullough, N., S. Dickenson, S. Schlechter, and J. Boland. 2007. "Centrifuge Seismic Modeling of Pile-Supported Wharves." *Geotechnical Testing Journal* 30, no. 5 (September): 349–359. https://doi.org/10.1520/GTJ14066

Nadim, F., G. Biscontin, and A. M. Kaynia. n.d. "Seismic Triggering of Submarine Slides." Paper presented at the Offshore Technology Conference, Houston, TX, April 30–May 3, 2007.

O'Leary, D. W. 1991. "Structure and Morphology of Submarine Slab Slides: Clues to Origin and Behaviour." *Marine Geotechnology* 10, nos. 1–2 (December): 53–69. https://doi.org/10.1080/10641199109379882

Oliveira, J. R. M. S., M. S. S. Almeida, H. P. G. Motta, and M. C. F. Almeida. 2011. "Influence of Penetration Rate on Penetrometer Resistance." *Journal of Geotechnical and Geoenvironmental Engineering* 137, no. 7 (July): 695–703. https://doi.org/10.1061/(ASCE)GT.1943-5606.0000480

Pestana, J. M. and F. Nadim. 2000. *Nonlinear Site Response Analysis of Submerged Slopes*, *Technical Report UCB/GT/2000-04*. Berkeley, CA: University of California, Berkeley.

Pirchiner, M., S. Drouet, M. Assumpção, J. Dourado, J. Ferreira, L. Vieira, and J. Juliá. n.d. "PSHAB: Probabilistic Seismic Hazard Analysis for Brazil: A National Hazard Map Building Effort." Paper presented at the 26th International Union of Geodesy and Geophysics General Assembly, Prague, Czech Republic, June 22-July 2, 2015.

Randolph, M. and S. Gourvenec. 2011. *Offshore Geotechnical Engineering*, 1st ed. Boca Raton, FL: CRC Press.

Rayhani, M. and M. H. El Naggar. 2007. "Centrifuge Modeling of Seismic Response of Layered Soft Clay." *Bulletin of Earthquake Engineering* 5, no. 4 (September): 571–589. https://doi.org/10.1007/s10518-007-9047-0

Rodríguez-Ochoa, R., F. Nadim, J. M. Cepeda, M. A. Hicks, and Z. Liu. 2015. "Hazard Analysis of Seismic Submarine Slope Instability." *Georisk: Assessment and Management of Risk for Engineered Systems and Geohazards* 9, no. 3 (August): 128–147. https://doi.org/10.1080/17499518.2015.1051546

Sathialingam, N. and B. Kutter. 1989. *The Effects of High Strain Rate and High Frequency Loading on Soil Behavior in Centrifuge Model Tests*, *NCEL Contract Report CR 89.011*. Port Hueneme, CA: Naval Civil Engineering Laboratory.

Sharma, J. S. and M. D. Bolton. 1996. "Centrifuge Modeling of an Embankment on Soft Clay Reinforced with Geogrid." *Geotextiles and Geomembranes* 14, no. 1 (January): 1–17. https://doi.org/10.1016/0266-1144(96)00003-9

Solheim, A., P. Bryn, H. P. Sejrup, J. Mienert, and K. Berg. 2005. "Ormen Lange—An Integrated Study for the Safe Development of a Deep-Water Gas Field within the Storegga Slide Complex, NE Atlantic Continental Margin; Executive Summary." *Marine and Petroleum Geology* 22, nos. 1–2 (January/February): 1–9. https://doi.org/10.1016/j.marpetgeo.2004.10.001

Soriano, C., R. B. Andrade, S. Mollepaza, M. S. S. Almeida, M. C. F. Almeida, J. R. M. Oliveira, and P. Trejo. n.d. "Simulation of a Weak Layered Profile Using Geotechnical Centrifuge." Paper presented at the XVI Pan-American Conference on Soil Mechanics and Geotechnical Engineering, Cancun, Mexico, November 17–20, 2019.

Springman, S. M. "Lateral Loading on Piles due to Simulated Embankment Construction." PhD diss., Cambridge University, 1989.

Stewart, D. P. and M. F. Randolph. 1991. "A New Site Investigation Tool for the Centrifuge." In *Centrifuge 91: Proceedings of the International Conference on Centrifuge Modeling*. Boca Raton, FL: CRC Press, 531–538.

Taboada, V. M. and R. Dobry. 1998. "Centrifuge Modeling of Earthquake Induced Lateral Spreading in Sand." *Journal of Geotechnical and Geoenvironmental Engineering* 124, no. 12 (December): 1995–1206. https://doi.org/10.1061/(ASCE)1090-0241(1998)124:12(1195)

Tarazona, S. F. M., M. C. F. Almeida, A. Bretschneider, M. S. S. Almeida, S. Escoffier, and R. G. Borges. 2020. "Evaluation Of Seismic Site Response of Submarine Clay Canyons Using Centrifuge Modelling." *International Journal of Physical Modelling in Geotechnics* 20, no. 4 (July): 224–238. https://doi.org/10.1680/jphmg.18.00084

Taylor, R. N. 1995. "Centrifuge Modelling: Principles and Scale Effects." In *Geotechnical Centrifuge Technology*, edited by R. N. Taylor. Boca Raton, FL: CRC Press, 19–33.

Tricarico, M., S. P. G. Madabhushi, and S. Aversa. 2016. "Centrifuge Modelling of Flexible Retaining Walls Subjected to Dynamic Loading." *Soil Dynamics and Earthquake Engineering* 88 (September): 297–306. https://doi.org/10.1016/j.soildyn.2016.06.013

Viggiani, G. and J. H. Atkinson. 1995. "Stiffness of Fine-Grained Soil at Very Small Strains." *Geotechnique* 45, no. 2 (June): 249–265. https://doi.org/10.1680/geot.1995.45.2.249

White, D. J., C. Gaudin, and N. Boylan. 2010. "Interpretation of T-Bar Penetrometer Tests at Shallow Embedment and in Very Soft Soils." *Canadian Geotechnical Journal* 47 (February): 218–219. https://doi.org/10.1139/T09-096

Williamson, M. "Tunnelling Effect on Bored Piles in Clay." PhD diss., University of Cambridge, 2014.

Wroth, C. P. 1984. "The Interpretation of In Situ Soil Tests." *Geotechnique* 34, no. 4 (December): 449–489. https://doi.org/10.1680/geot.1984.34.4.449

Zhang, C., D. White, and M. Randolph. 2011. "Centrifuge Modeling of the Cyclic Lateral Response of a Rigid Pile in Soft Clay." *Journal of Geotechnical and Geoenvironmental Engineering* 137, no. 7 (July): 717–729. https://doi.org/10.1061/(ASCE)GT.1943-5606.0000482

Zhou, Y.-G., J. Chen, Y.-M. Chen, B. L. Kutter, B.-L. Zheng, D. W. Wilson, M. E. Stringer, and E. C. Clukey. 2017. "Centrifuge Modeling and Numerical Analysis on Seismic Site Response of Deep Offshore Clay Deposits." *Engineering Geology* 227 (September): 54–68. https://doi.org/10.1016/j.enggeo.2017.01.008

Zhou, Y.-G., J. Chen, Y. She, A. M. Kaynia, B. Huang, and Y.-M. Chen. 2017. "Earthquake Response and Sliding Displacement of Submarine Sensitive Clay Slopes." *Engineering Geology* 227 (September): 69–83. https://doi.org/10.1016/j.enggeo.2017.05.004